YALE JOURNAL OF BIOLOGY AND MEDICINE 96 (2023), pp.383-396.

CASE REPORT

YALE JOURNAL OF BIOLOGY AND MEDICINE
YJBM
CELEBRATING 95 YEARS 1928–2023

A Stop-gain Variant c.220C>T (p.(Gln74*)) in *FLNB* Segregates with Spondylocarpotarsal Synostosis Syndrome in a Consanguineous Family

Hamna Shahid[a,1], Nazish Shakoor[b,1], Anisa Bibi[b], Asma Saleem Qazi[a], Rida Fatima Saeed[a], Aqeela Nawaz[b], Sajid Malik[b,*], and Sara Mumtaz[a,*]

[a]*Department of Biological Sciences, National University of Medical Sciences, Rawalpindi, Pakistan;* [b]*Human Genetics Program, Department of Zoology, Faculty of Biological Sciences, Quaid-i-Azam University, Islamabad, Pakistan*

Spondylocarpotarsal synostosis (SCT) syndrome is a very rare and severe form of skeletal dysplasia. The hallmark features of SCT are disproportionate short stature, scoliosis, fusion of carpal and tarsal bones, and clubfoot. Other common manifestations are cleft palate, conductive and sensorineural hearing loss, joint stiffness, and dental enamel hypoplasia. Homozygous variants in *FLNB* are known to cause SCT. This study was aimed to investigate the phenotypic and genetic basis of unique presentation of SCT syndrome segregating in a consanguineous Pakistani family. Three of the four affected siblings evaluated had severe short stature, short trunk, short neck, kyphoscoliosis, pectus carinatum, and winged scapula. The subjects had difficulty in walking and gait problems and complained of knee pain and backache. Roentgenographic examination of the eldest patient revealed gross anomalies in the axial skeleton including thoracolumbar and cervical fusion of ribs, severe kyphoscoliosis, thoracic and lumbar lordosis, coxa valga, fusion of certain carpals and tarsals, and clinodactyly. The patients had normal faces and lacked other typical features of SCT like cleft palate, conductive and sensorineural hearing loss, joint stiffness, and dental enamel hypoplasia. Whole exome sequencing (WES) of two affected siblings led to the discovery of a rare stop-gain variant c.220C>T (p.(Gln74*)) in exon 1 of the *FLNB* gene. The variant was homozygous and segregated with the malformation in this family. This study reports extensive phenotypic variability in SCT and expands the mutation spectrum of *FLNB*.

*To whom all correspondence should be addressed: Dr. Sara Mumtaz, PhD, Human Genetics Section, National University of Medical Sciences, Rawalpindi, Pakistan; Email: sara.mumtaz@numspak.edu.pk; ORCID: 0000-0003-0503-1060. Prof. Dr. Sajid Malik, PhD, Human Genetics Program, Department of Zoology, Quaid-i-Azam University, Islamabad, Pakistan; Email: malik@qau.edu.pk; ORCID: 0000-0001-5563-9053.

Abbreviations: AO, Atelosteogenesis; AOI, atelosteogenesis I; BD, Boomerang dysplasia; FLNB, Filamin B gene; MSS, Multiple synostosis syndrome; OMIM, Mendelian inheritance in Man; SCT, Spondylocarpotarsal synostosis; WES, whole exome sequencing.

Keywords: short stature, kyphoscoliosis, carpal and tarsal fusion, pectus carinatum, winged scapula, lordosis, coxa valga

Author Contributions: SMk and SMz contributed to conceptualization and supervision. NS and SMk performed clinical investigations; HS, ASQ, AB, RFS, and AN performed genetic studies and bioinformatics analysis. SMk and SMz wrote and revised the manuscript. All authors gave final approval and agreed to be accountable for all aspects of the work.

[1]Contributed equally: HS and NS.

INTRODUCTION

Exome sequencing has made it possible to identify causal mutations in a variety of varied and complex illnesses, according to several recent studies [1,2]. In skeletal dysplasias, patients may be in a critical condition and have a phenotypically complex presentation; confirming a conclusive molecular diagnosis in such cases is frequently challenging and expensive. Using conventional methods like Sanger sequencing is not just expensive but also very time-consuming. Because skeletal dysplasias are clinical and genetically heterogeneous disorders, gene-by-gene sequencing is sometimes impractical. Simultaneous analysis of all genes by whole exome sequencing (WES) is a more practical approach. Exome sequencing has the additional advantage of not needing prior knowledge of the genes causing a medical condition [3].

The actin-binding protein FLNB, which is produced by the human *FLNB* gene on chromosome 3p14.3, is hypothesized to transmit signals from different membrane receptors and intracellular proteins onto the actin cytoskeleton. It controls cell proliferation, differentiation, and migration that are cytoskeleton-dependent [4]. In 2004 a novel study reported homozygous and heterozygous *FLNB* mutations in four human skeletal disorders including spondylocarpotarsal syndrome (SCT, OMIM 272460), the perinatal lethal atelosteogenesis I and III phenotypes (AOI, OMIM 108720; AOIII, OMIM 108721), and Larsen syndrome (LS, OMIM 150250) [5]. Later on, it was found that Boomerang dysplasia (BD; OMIM 112310) is also caused by mutations in this gene [6]. Loss of function mutations were found in cases of autosomal recessive SCT while gain of function mutations were found in autosomal dominant AOI, AOIII, and BD and Larsen syndrome [4].

Spondylocarpotarsal synostosis syndrome (SCT) is characterized by spinal deformity and disproportionately short stature. Clinical characteristics comprise conductive hearing loss, facial dysmorphism, cleft palate, dental enamel hypoplasia, clubbed feet, and joint laxity (Table 1). Block vertebrae and the fusion of the carpal and tarsal bones are typical radiologic findings. Epiphyseal dysplasia of the femur and a delay in the ossification of the carpal bones' epiphyses have both been noted [7].

In the present study, we had a familial case of complex skeletal dysplasia and clinicians were not able to give an accurate diagnosis just based on clinical presentation. Therefore, we performed whole exome sequencing (WES) and identified a variant in the Filamin B gene (*FLNB*) that segregated in the family and likely causes the phenotype.

CASE PRESENTATION

Family Recruitment and Pedigree

All information and biological material were collected according to the Helsinki II declaration. The approval of the study was taken by ethical review boards of Quaid-i-Azam University and National University of Medical Sciences, Rawalpindi, Pakistan. The family originates from a rural area of northern Pakistan. A four-generation pedigree drawn with the help of family elders strongly illustrated autosomal recessive pattern of inheritance (Figure 1A). The unaffected parents had a consanguineous union and there were four affected siblings of which one was deceased in early childhood.

Clinical Presentation

The parents and two unaffected siblings physically examined were free of any musculoskeletal or limb malformation. The patients had disproportionately short stature with short trunks and short necks (Figure 1B; Table 2). The elder patients 405 and 407 had kyphoscoliosis, protruding sternum and abdomen, and winged scapula. They had round faces, mild frontal bossing, and otherwise unremarkable facial features.

The subjects have difficulty in walking and problems with gait. Patients complained of knee pain and backache. The eldest patient 405 had the most severe symptoms while 408 had a mild appearance. Reportedly, one of the deceased patients 404 also had severe symptoms. According to the parents, the patients appear asymptomatic at birth. The malformation was progressive and symptoms appeared in 5-6 months of infancy. They all have normal IQ, hearing, and vision. All patients were attending a normal school. Anthropometric measurements showed severe short stature and failure to achieve developmental landmarks (Table 3).

Radiological Observations

Roentgenographic examination of eldest patient 405 revealed gross anomalies in the axial skeleton including thoracolumbar fusions, cervical fusion of ribs, kyphoscoliosis, and thoracic and lumbar lordosis (Figure 1C). There were pelvic girdle anomalies, including sacral agenesis and coxa valga. There was delayed epiphyseal maturation on all the long bones. In the upper limbs, there was carpal synostosis remarked as capitate-hamate coalition and lunate-triquetrum fusion. There was clinodactyly more pronounced in the right hand, however, there was no shortening of metacarpals. In the lower limbs, there was fusion of tarsal bones. The patient had generalized delayed bone age.

Genetic Findings

Two affected individuals, 405 and 407, underwent

Table 1. Comparison of Clinical Features of SCT Syndrome Patients Having Biallelic *FLNB* Variants

Study	Krakow et al. 2004 [9]	Farrington-Rock et al. 2007 [10]	Brunetti-Pierri et al. (2008)	Mitter et al. 2008 [11]	Yang et al. 2017 [1]	Salian et al. 2018 [3]	Yasin et al. 2021	Fukushima et al. 2021	This study	Summary of features
Variant	c.1945C>T; c.2452C>T; c.4819C>T; c.6408delC; c.7029T>G	c.4671G>A; c.5548G>T	c.5548G>T	c.6010C>T	c.7621dupG	c.28G>T; c.429delinsCT; c.1204delG; c.1243C>T; c.1493delA; c.1592dup; c.6317delC	c.2911dupG	c.1346-1372_1941+389del; c.3127-353_4223-1836del	c.220C>T	
Gender (M:F)	5:6	2:0	0:1	1:0	0:2	6:4	3:2	1:1	2:1	20:17
Short stature	11/11	2/2	1/1	1/1	2/2	10/10	5/5	2/2	3/3	100%
Short neck	9/11	2/2	1/1	1/1	2/2	6/10	5/5	2/2	3/3	83%
Carpal fusion	11/11	NR	1/1	1/1	2/2	9/10	4/5	2/2	2/2	94%
Scoliosis	11/11	2/2	1/1	1/1	2/2	9/10	3/5	2/2	3/3	92%
Lordosis	NR	NR	1/1	0/1	2/2	2/10	3/5	2/2	2/2	52%
Vertebral fusion	+	+	+	+	+	+	+	+	+	100%
Delayed bone age	+	+	+	+	+	+	+	+	+	100%
Facial deformities	11/11	NR	NR	1/1	0/2	3/10	3/5	NR	0/3	56%
Tarsal fusion	7/11	NR	1/1	NR	0/2	3/10	3/5	1/2	2/2	52%
Hearing deficit	7/11	NR	NR	1/1	1/2	2/10	1/5	2/2	0/3	41%
Enamel hypoplasia	7/11	NR	NR	NR	0/2	NR	0/5	NR	0/3	33%

NR: Not reported; +, feature present in family/subject.

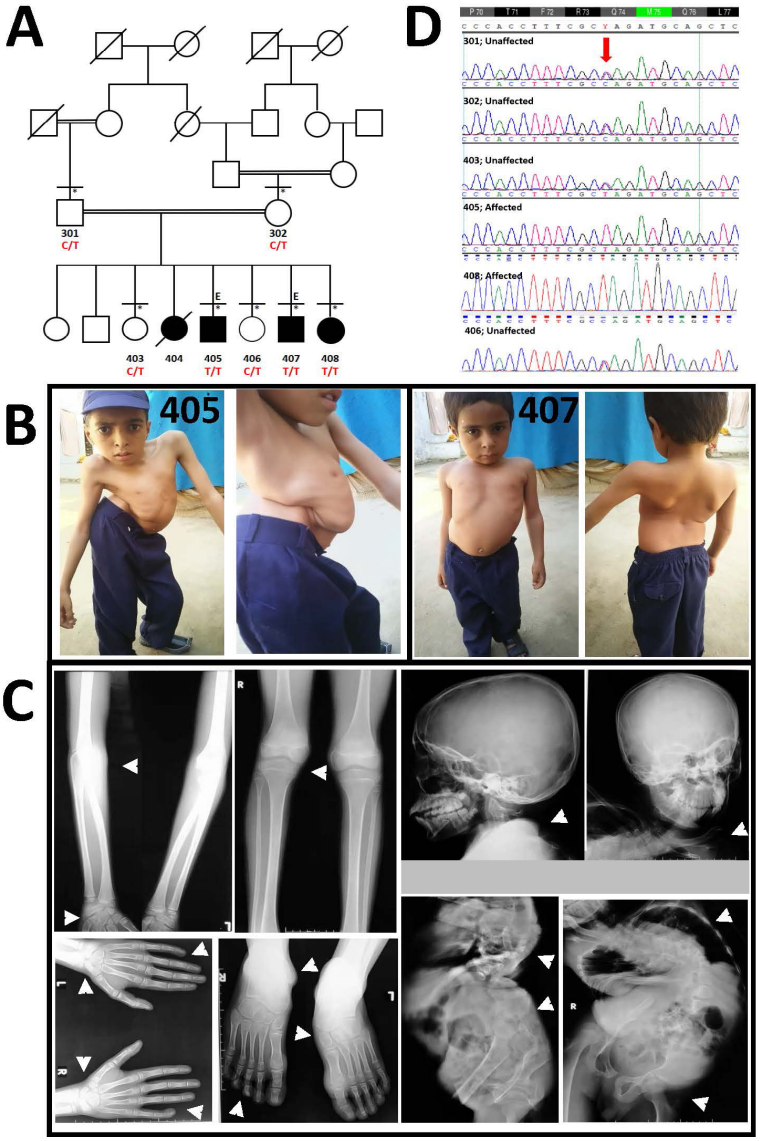

Figure 1. **A**. **Pedigree of the family**. Horizontal lines above individuals indicate that physical examination was performed. *indicates subjects participated in genetic study; "E," subjects underwent WES. **B**. Phenotype in affected subjects 405 and 407. **C**. Roentgenographic examination of 405. **D**. Electropherograms showing the segregation of identified variant c.220C>T in *FLNB*.

whole exome sequencing (WES). The standard filtration scheme of the exome data (as per [8-10]) showed 28 rare exonic, homozygous, and nonsynonymous variants shared by the two affected subjects (Appendix A: Supplemental Table 1). Among those, only the variant c.220C>T (p.(Gln74*)) in exon 1 of *FBLN* (NM_001164317) was the best candidate. Sanger sequencing confirmed the segregation of the variant with the malformation (Figure 1D). This variant is extremely rare and no homozygous form has been reported so far (only two alleles out of 251,294 in global diversity panel with allele frequency 7.96 x 10^{-6} and in South Asian population, only two alleles in the heterozygous state out of 30,602). This variant showed complete conservation in deep phylogenetic analyses (Vertebrate Multiz Alignment & Conservation Track of UCSC Genome Browser; Supplemental Figure 1).

DISCUSSION

The characteristic features in our patients were postnatal disproportionate short stature, scoliosis, and lordosis. As a differential diagnosis, we considered Larsen syndrome (OMIM 150250), atelosteogenesis type I (OMIM 108720), multiple synostosis syndrome (MSS; OMIM 186500), Klippel-Feil syndrome 1 (OMIM 118100), and spondylocostal dysplasia (OMIM 277300). The malfor-

Table 2. Phenotypic Variability in Patients

Subject ID	405	407	408	Feature reported in OMIM
Sex, age (years)	M, 12	M, 10	F, 8	
Structural features				
Short stature, disproportionate	+	+	+	+
Short neck	+	+	+	+
Short trunk	+	+	+	+
Kyphoscoliosis	+	+	–	+
Winged scapulae	+	+	–	+
Crowded ribs	+	+	–	+
Cervical fusion of ribs	+	NA	NA	+
Pectus carinatum	+	+	–	+
Thoracolumbar fusions	+	NA	NA	+
Thoracic and lumbar lordosis	+	NA	NA	+
Protruding abdomen (secondary to lordosis)	+	+	–	+
Pelvic girdle anomalies and coxa valga	+	NA	NA	+
Joint laxity	+	+	+	+
Craniofacial				
Dysmorphic face	–	–	–	–
Face type	Round	Round	Round	
Frontal bossing, mild	+	+	+	+
Hearing loss, conductive	–	–	–	+
Ocular findings	–	–	–	+
Anteverted nares	–	–	–	+
Tooth enamel hypoplasia	–	–	–	+
Failure of eruption of permanent teeth	–	–	–	+
High arched palate	–	–	–	+
Cleft palate	–	–	–	+
Limb				
Clinodactyly	+	–	–	+
Brachydactyly	–	–	–	+
Clubfoot	–	–	–	+
Flat foot	+	+	+	+
Delayed epiphyseal maturation	+	NA	NA	+
Carpal and tarsal synostosis	+	NA	NA	+

+, feature present; –, feature absent; NA, not assessed.

mation in the present family is different from Larsen syndrome because of the absence of certain features like congenital dislocations of the hip, knee, elbow, and shoulder, depressed nasal bridge, and widely spaced eyes. The condition in our patients is also distinct from atelosteogenesis type I which is characterized by perinatal lethal short-limbed dwarfism and severe dislocated hips, knees, and elbows. Multiple synostosis syndrome (MSS) shares features of vertebral dysplasia with our family but could be excluded because of progressive symphalangism and distinct facial findings in multiple synostosis. MSS segregates as an autosomal dominant entity. Further, Klippel-Feil syndrome 1 which segregates autosomal dominantly, generally does not show carpal or tarsal fusions, instead, there are isolated cervical fusions which do not occur in SCT syndrome. Another vertebral malformation,

Table 3. Anthropometric Measurements of Affected Siblings

Features	405	407	408
Sex, age (years)	M, 12	M, 10	F, 8
Standing height*	85 (–5)	83 (–5)	62 (–5)
Sitting height†	49 (–4)	54 (–3.5)	43 (–3.5)
Arm span§	86 (–3.5)	92 (–3.5)	78 (–3.5)
Head circumference‡	54 (+0.5)	53 (+0.25)	48 (–2)
Chest circumference	48	57	43

Standard deviations are given in parentheses. All measurements are in cm. Head circumference is with respect to age and sex. Arm span is with reference to height. *Standard deviations are from WHO Growth Reference: http://www.who.int/growthref/who2007_height_for_age/en/. †Kelly AM, Shaw NJ, Thomas AM, Pynsent PB, Baker DJ. Growth of Pakistani children in relation to the 1990 growth standards. Arch Dis Child. 1997;77:401-5. §Chen WY, Lin YT, Chen Y, Chen KC, Kuo BI, Tsao PC, Lee YS, Soong WJ, Jeng MJ. Reference equations for predicting standing height of children by using arm span or forearm length as an index. J Chin Med Assoc. 2018;81:649-56. ‡James HE, Perszyk AA, MacGregor TL, Aldana PR. The value of head circumference measurements after 36 months of age: a clinical report and review of practice patterns. J Neurosurg Pediatr. 2015;16(2):186-94.

ie, spondylocostal dysplasia also accompanies rib anomalies different from SCT. Finally, the candidate genes for the aforementioned syndromes (i.e., *DLL3, FGF9, GDF5, GDF6, HES7, LFNG, MESP2, MYH3, NOG, RIPPLY2,* and *TBX6*) were excluded for any rare pathogenic variant in the exome data analyses.

The malformation in this family was presented with disproportionate short stature with short trunk and short neck, kyphoscoliosis, protruding sternum and abdomen, and winged scapula. The malformation was progressive and severity was increasing with age. The patients had rather unremarkable facial features, and normal IQ, hearing, and vision. The roentgenographic study revealed characteristic gross anomalies in the axial skeleton including thoracolumbar fusions, cervical fusion of ribs, kyphoscoliosis, thoracic and lumbar lordosis, pelvic girdle anomalies and coxa valga, delayed epiphyseal maturation of long bones, and carpal and tarsal synostosis. However, other features of SCT such as hearing loss, visual anomalies, anteverted nares, tooth enamel hypoplasia, failure of eruption of permanent teeth, high arched palate and cleft palate, and brachydactyly were not witnessed among the affected subjects (Table 2). This unusual combination cautioned further molecular genetic investigations. Hence, in order to reach a correct molecular diagnosis, WES was launched which led to the detection of c.220C>T (p.(Gln74*)) in exon 1 of *FBLN*. No other rare pathogenic variant in genes related to skeletal morphogenesis was detected in the exome data.

FLNB is known to be associated with several allelic disorders. Heterozygous variants in *FLNB* are known to cause at least four autosomal dominant anomalies, ie, AOI, AOIII, BD, and LS [3-6]. Most of these variants are missense and tend to be clustered in actin-binding domains and repeat domains 13–15 of FLNB and are predicted to cause gain-of-function (GOF). GOF may exert their effect through various mechanisms such as constitutive or ectopic activation, shift of substrate or binding target specificity, or protein aggregation [11]. Recently, Huang et al. reported two heterozygous variants (c.1321C>CA and c.1693C>A) in two different families with nonsyndromic clefts of lip/palate [12]. The authors argued that the variants resulted in loss-of-function. Heterozygous variants in FLNB were also reported in isolated congenital talipes equinovarus and osteochondrodysplasia (Piepkorn type) [13,14]. On the other hand, homozygous or compound heterozygous missense, nonsense or frameshift truncating variants are known to cause recessively inherited SCT syndrome [7]. SCT associated variants generally affect FLNB actin-binding domains and repeat domains. Nonsense or frameshift variants in FLNB generally result in the truncated version or absence of the encoded protein which is because of nonsense-mediated decay of mRNA and result in loss of function (LOF) [15]. The LOF mutations are predicted to cause impairment of protein, preventing its production or decrease the activity of the product [16]. At least 20 pathogenic variants in *FLNB*, mostly in homozygous state, have been shown to be segregating in SCT syndrome families (Appendix B: Supplemental Table 2).

In the present family, heterozygotes were asymptomatic. Curiously however, one of the heterozygous carriers in the family reported by Yasin et al. exhibited mild short stature [17]. The authors remarked that this may indicate a semi-dominant less severe heterozygous effect of the variant or co-inheritance of pathogenic variants in other genes. However, they did not report any second candidate variant likely contributing to the phenotype. Among all the reported variants, the variant in the present family is causing most early termination in the reading frame. This may explain the severe skeletal manifestations in our family.

Farrington-Rock et al. and Lu et al. independently generated *Flnb* deficient mice and shed light in the

role of *FLNB* gene in skeletal development [18,19]. In the experience of Farrington-Rock et al. a remarkable similarity was observed between this mouse model and human SCT syndrome [18]. Skeletal abnormalities and short stature and fusion of neural arches of the vertebrae in the cervical and thoracic spine of newborn *Flnb*$^{-/-}$ mice were evident. The authors further showed that the *Flnb* deficient mice had progressive vertebral fusions, which is contrary to the previous hypothesis that SCT results from failure of normal spinal segmentation. Hence, the authors proposed that spinal segmentation can occur normally in the absence of filamin B, but the protein is required for maintenance of intervertebral, carpal and sternal joints, and the joint fusion process commences antenatally. Concordantly, Lu et al. also demonstrated that *Flnb* deficient mice have developed fusion of the ribs and vertebrae, abnormal spinal curvatures, and dysmorphic facial/calvarial bones, similar to the human phenotype [19]. In addition, *Flnb*$^{-/-}$ also exhibited shortened distal limbs with small body size. These minor differences between the phenotypes of *Flnb*$^{-/-}$ mice generated by Lu et al. and Farrington-Rock et al. could be due to the use of different sizes of clones, vectors, cell lines, transfection methods, and the genetic background of mice, in addition to other stochastic factors.

In vertebrate species, morphogenesis necessitates the fusion of extracellular signals with modifications to the cytoskeleton. Cytoskeletal F-actin is organized by filaments into orthogonal gel networks or parallel bundles [20]. Additionally, filamins mediate connections between transmembrane receptors and subcortical actin networks to modify cell-matrix, cell-cell, and intracytoplasmic signal transduction [5]. Three filamin genes, *FLNA*, *FLNB*, and *FLNC*, are present in mammals. The expression of *FLNA* and *FLNB* appears to be widespread while *FLNC* expression is seen mainly in the muscle [21,22]. The wide range of skeletal defects brought on by *FLNB* mutations suggests that filamin B plays a crucial function in skeletal development.

CONCLUSION

The malformation in our family was molecularly diagnosed as SCT syndrome and hence it supports the published reports. We identified a very rare stop-gain variation c.220C>T (p.(Gln74*)) in the first exon of the *FLNB* gene causing a very early termination of the reading frame and hence, explaining a rather severe skeletal manifestation in this family. This expands the mutation spectrum of the *FLNB* gene. Our results will help in the genetic counseling of affected families to prevent reoccurrence of disease in future generations.

Acknowledgments: We graciously acknowledge the participation of the family in this study and the physicians for clinical assessment of the family.

Data Availability: The datasets generated during and/or analyzed during the current study are available from the corresponding author on reasonable request.

Grants: This work was supported by URF-QAU, Pakistan [DFBS/2014/3230, 2013-2014] and HEC, Pakistan.

Conflict of Interest: No financial or non-financial benefits have been received or will be received from any party related directly or indirectly to the subject of this article.

REFERENCES

1. Marinakis NM, Svingou M, Veltra D, Kekou K, Sofocleous C, Tilemis FN, et al. Phenotype-driven variant filtration strategy in exome sequencing toward a high diagnostic yield and identification of 85 novel variants in 400 patients with rare Mendelian disorders. Am J Med Genet A. 2021 Aug;185(8):2561–71.
2. Negri G, Magini P, Milani D, Crippa M, Biamino E, Piccione M, et al. Exploring by whole exome sequencing patients with initial diagnosis of Rubinstein-Taybi syndrome: the interconnections of epigenetic machinery disorders. Hum Genet. 2019 Mar;138(3):257–69.
3. Jeon GW, Lee MN, Jung JM, Hong SY, Kim YN, Sin JB, et al. Identification of a de novo heterozygous missense FLNB mutation in lethal atelosteogenesis type I by exome sequencing. Ann Lab Med. 2014 Mar;34(2):134–8.
4. Hu J, Lu J, Lian G, Ferland RJ, Dettenhofer M, Sheen VL. Formin 1 and filamin B physically interact to coordinate chondrocyte proliferation and differentiation in the growth plate. Hum Mol Genet. 2014 Sep;23(17):4663–73.
5. Krakow D, Robertson SP, King LM, Morgan T, Sebald ET, Bertolotto C, et al. Mutations in the gene encoding filamin B disrupt vertebral segmentation, joint formation and skeletogenesis. Nat Genet. 2004 Apr;36(4):405–10.
6. Bicknell LS, Morgan T, Bonafé L, Wessels MW, Bialer MG, Willems PJ, et al. Mutations in FLNB cause boomerang dysplasia. J Med Genet. 2005 Jul;42(7):e43–43.
7. Salian S, Shukla A, Shah H, Bhat SN, Bhat VR, Nampoothiri S, et al. Seven additional families with spondylocarpotarsal synostosis syndrome with novel biallelic deleterious variants in FLNB. Clin Genet. 2018 Jul;94(1):159–64.
8. Shabbir RM, Nalbant G, Ahmad N, Malik S, Tolun A. Homozygous CHST11 mutation in chondrodysplasia, brachydactyly, overriding digits, clino-symphalangism and synpolydactyly. J Med Genet. 2018 Jul;55(7):489–96.
9. Koprulu M, Kumare A, Bibi A, Malik S, Tolun A. The first adolescent case of Fraser syndrome 3, with a novel nonsense variant in GRIP1. Am J Med Genet A. 2021 Jun;185(6):1858–63.
10. Naqvi SF, Shabbir RM, Tolun A, Basit S, Malik S. A Two-Base Pair Deletion in IQ Repeats in ASPM Underlies Microcephaly in a Pakistani Family. Genet Test Mol Biomarkers. 2022 Jan;26(1):37–42.
11. Stenson PD. P. D. et al. "The Human Gene Mutation

Database: towards a comprehensive repository of inherited mutation data for medical research, genetic diagnosis and next-generation sequencing studies. Volume 136. Human Genetics; 2017. pp. 665–77.
12. Huang W, Zhang S, Lin J, Ding Y, Jiang N, Zhang J, et al. Rare loss-of-function variants in FLNB cause non-syndromic orofacial clefts. J Genet Genomics. 2023 Mar;31:S1673–8527.
13. Yang H, Zheng Z, Cai H, Li H, Ye X, Zhang X, et al. Three novel missense mutations in the filamin B gene are associated with isolated congenital talipes equinovarus. Hum Genet. 2016 Oct;135(10):1181–9.
14. Rehder H, Laccone F, Kircher SG, Schild RL, Rapp C, Bald R, et al. Piepkorn type of osteochondrodysplasia: defining the severe end of FLNB-related skeletal disorders in three fetuses and a 106-year-old exhibit. Am J Med Genet A. 2018 Jul;176(7):1559–68.
15. Yang CF, Wang CH, Siong H'ng W, Chang CP, Lin WD, Chen YT, et al. Filamin B loss-of-function mutation in dimerization domain causes autosomal recessive Spondylocarpotarsal Synostosis syndrome with rib anomalies. Hum Mutat. 2017 May;38(5):540–7.
16. Gerasimavicius L, Livesey BJ, Marsh JA. Loss-of-function, gain-of-function and dominant-negative mutations have profoundly different effects on protein structure. Nat Commun. 2022 Jul;13(1):3895.
17. Yasin S, Makitie O, Naz S. Spondylocarpotarsal synostosis syndrome due to a novel loss of function FLNB variant: a case report. BMC Musculoskelet Disord. 2021 Jan;22(1):31.
18. Farrington-Rock C, Kirilova V, Dillard-Telm L, Borowsky AD, Chalk S, Rock MJ, et al. Disruption of the Flnb gene in mice phenocopies the human disease spondylocarpotarsal synostosis syndrome. Hum Mol Genet. 2008 Mar;17(5):631–41.
19. Lu J, Lian G, Lenkinski R, De Grand A, Vaid RR, Bryce T, et al. Filamin B mutations cause chondrocyte defects in skeletal development. Hum Mol Genet. 2007 Jul;16(14):1661–75.
20. Niederman R, Amrein PC, Hartwig J. Three-dimensional structure of actin filaments and of an actin gel made with actin-binding protein. J Cell Biol. 1983 May;96(5):1400–13.
21. Gorlin JB, Yamin R, Egan S, Stewart M, Stossel TP, Kwiatkowski DJ, et al. Human endothelial actin-binding protein (ABP-280, nonmuscle filamin): a molecular leaf spring. J Cell Biol. 1990 Sep;111(3):1089–105.
22. Takafuta T, Wu G, Murphy GF, Shapiro SS. Human β-filamin is a new protein that interacts with the cytoplasmic tail of glycoprotein Ibalpha. J Biol Chem. 1998 Jul;273(28):17531–8.

Chr	Start	End	Ref	Alt	Func.refGe	Gene.refGe	GeneDetail	ExonicFunc	AAChange.	cytoBand	ExAC_ALL	ExAC_AFR
chr1	13223492	13223492	A	G	exonic	PRAMEF18	.	nonsynony	PRAMEF18	1p36.21	.	.
chr1	13223511	13223511	T	C	exonic	PRAMEF18	.	nonsynony	PRAMEF18	1p36.21	.	.
chr1	13223511	13223511	T	C	exonic	PRAMEF18	.	nonsynony	PRAMEF18	1p36.21	.	.
chr1	1.2E+08	1.2E+08	T	G	exonic	NBPF8	.	nonsynony	NBPF8:NM	1p11.2	.	.
chr1	1.49E+08	1.49E+08	T	C	exonic	NBPF9	.	nonsynony	NBPF9:NM	1q21.2	.	.
chr10	45826906	45826906	G	C	exonic	AGAP4	.	nonsynony	AGAP4:NM	10q11.22	.	.
chr10	87234695	87234695	G	A	exonic	NUTM2A	.	nonsynony	NUTM2A:N	10q23.2	0	.
chr10	95068566	95068566	T	C	splicing	CYP2C8	NM_00119	.	.	10q23.33	.	.
chr11	1629969	1629969	-	GGCTGTGC	exonic	KRTAP5-5	.	nonframes	KRTAP5-5:I	11p15.5	0.0065	0.0261
chr11	71527629	71527629	-	CTGCTGCC	exonic	KRTAP5-7	.	nonframes	KRTAP5-7:I	11q13.4	.	.
chr11	1.24E+08	1.24E+08	C	G	exonic	OR8G1	.	stopgain	OR8G1:NM	11q24.2	.	.
chr11	1.25E+08	1.25E+08	G	A	exonic	ROBO4	.	nonsynony	ROBO4:NM	11q24.2	0.0052	0.0004
chr13	1.13E+08	1.13E+08	G	A	exonic	LOC10192	.	nonsynony	LOC10192	13q34	.	.
chr18	63712604	63712604	G	T	exonic	SERPINB11	.	stopgain	SERPINB11	18q21.33	.	.
chr19	7032419	7032419	G	C	exonic	MBD3L5	.	nonsynony	MBD3L5:N	19p13.2	.	.
chr19	44477666	44477666	G	C	exonic	ZNF180	.	nonsynony	ZNF180:NM	19q13.31	.	.
chr19	44479350	44479350	G	C	exonic	ZNF180	.	nonsynony	ZNF180:NM	19q13.31	.	.
chr19	44497294	44497294	A	G	exonic	ZNF180	.	nonsynony	ZNF180:NM	19q13.31	.	.
chr2	1.12E+08	1.12E+08	C	A	exonic	RGPD5;RGI	.	nonsynony	RGPD8:NM	2q14.1	.	.
chr20	18630471	18630471	G	T	exonic	DTD1	.	nonsynony	DTD1:NM_	20p11.23	.	.
chr21	46152330	46152330	G	A	exonic	FTCD-AS1	.	nonsynony	FTCD-AS1:I	21q22.3	.	.
chr22	15528913	15528913	C	T	exonic	OR11H1	.	nonsynony	OR11H1:NI	22q11.1	1.65E-05	0
chr22	16783675	16783675	G	T	exonic	XKR3	.	nonsynony	XKR3:NM_(	22q11.1	.	.
chr22	16784234	16784234	A	C	exonic	XKR3	.	nonsynony	XKR3:NM_(	22q11.1	0.0037	0.0094
chr22	25039061	25039061	G	T	exonic	KIAA1671	.	nonsynony	KIAA1671:I	22q11.23	.	.
chr3	58008784	58008784	C	T	exonic	FLNB	.	stopgain	FLNB:NM_(	3p14.3	.	.
chr7	76533992	76533992	T	A	exonic	SPDYE16	.	nonsynony	SPDYE16:N	7q11.23	.	.
chr9	39358957	39358957	C	T	exonic	SPATA31A1	.	nonsynony	SPATA31A1	9p12	.	.

Appendix A: Supplemental Table 1. List of shared, rare homozygous variants in two exomes.

ExAC_AMR	ExAC_EAS	ExAC_FIN	ExAC_NFE	ExAC_OTH	ExAC_SAS	avsnp150	DamagePre	SIFT_pred	SIFT4G_pre	Polyphen2_	Polyphen2_	LRT_pred
.	.	.	.	.	.	rs5566717	0.1	.	.	.	.	.
.	.	.	.	.	.	rs2860987	0.1	.	.	.	.	.
.	.	.	.	.	.	rs2860987	0.1	.	.	.	.	.
.	.	.	.	.	.	rs3882061	.	.	.	.	.	.
.	.	.	.	.	.	rs7781487	0.2	.	T	.	.	.
.	.	.	.	.	.	.	1.2	T	T	B	B	N
.	.	.	.	.	.	rs1995307	0.18	T	T	B	B	N
.	.	.	.	.	.	rs2071426	.	.	.	.	.	.
0.0031	0.0009	0.0011	0.0098	0.0135	0.0009	rs7102576	.	.	.	.	.	.
.	.	.	.	.	.	.	.	.	.	.	.	.
.	.	.	.	.	.	rs4268525	0	.	.	.	.	.
0.0029	0.0003	0.0011	0.0045	0.0092	0.0169	rs1462767	1.19	T	T	B	B	N
.	.	.	.	.	.	rs9603837	1.4	.	D	.	.	.
.	.	.	.	.	.	rs4940595	0	.	.	.	.	.
.	.	.	.	.	.	rs8792092	7.19	D	D	D	D	D
.	.	.	.	.	.	rs1897820	1.3	.	D	.	.	.
.	.	.	.	.	.	rs2253563	1.3	.	D	.	.	.
.	.	.	.	.	.	rs2571108	0.3	.	T	.	.	.
.	.	.	.	.	.	rs7122775	0.19	T	T	B	B	.
.	.	.	.	.	.	rs6045525	0.3	.	.	.	.	.
.	.	.	.	.	.	rs4819208	.	.	.	.	.	.
0	0	0	3.00E-05	0	0	rs7835071	5.16	D	D	.	.	D
.	.	.	.	.	.	rs5748622	0.17	T	.	P	B	U
0.0019	0.0046	0	0.0045	0.0086	0	rs5748623	0.18	T	T	B	B	N
.	.	.	.	.	.	rs7315798	0.19	T	T	B	B	N
.	.	.	.	.	.	.	6.6	.	.	.	.	D
.	.	.	.	.	.	rs1754169	0.5	.	T	.	.	.
.	.	.	.	.	.	rs1012516	0.12	.	T	.	.	N

MutationTa	MutationA	FATHMM_I	PROVEAN_	VEST4_sco	MetaSVM_	MetaLR_pr	M-CAP_pre	REVEL_sco	MutPred_s	MVP_score	MPC_score	PrimateAI_
.	.	.	.	.	.	.	.	.	.	.	.	.
.	.	.	.	.	.	.	.	.	.	.	.	.
.	.	.	.	.	.	.	.	.	.	.	.	.
.	.	.	.	.	.	.	.	.	.	.	.	.
.	.	.	.	0.059	.	.	.	.	.	.	.	.
N	N	T	N	0.072	T	T	D	0.179	0.296	0.03	.	T
P	.	T	N	0.05	T	T	.	0.034	.	.	.	T
.	.	.	.	.	.	.	.	.	.	.	.	.
.	.	.	.	.	.	.	.	.	.	.	.	.
.	.	.	.	.	.	.	.	.	.	.	.	.
.	.	.	.	0.073	.	.	.	.	.	.	.	.
N	L	T	N	0.134	T	T	.	0.068	.	0.727	0.312	T
.	.	.	.	0.037	.	.	.	.	.	.	.	.
.	.	.	.	0.36	.	.	.	.	.	.	.	.
N	M	.	D	0.691	T	T	T	0.094	.	.	.	T
.	.	.	.	0.204	.	.	.	.	.	.	.	.
.	.	.	.	0.191	.	.	.	.	.	.	.	.
.	.	.	.	0.064	.	.	.	.	.	.	.	.
N	N	T	N	0.05	T	T	T	0.039	.	0.03	.	T
P	.	.	.	.	.	.	.	.	.	.	.	.
.	.	.	.	.	.	.	.	.	.	.	.	.
.	.	T	D	0.323	T	T	T	0.05	.	0.474	.	T
P	N	T	N	0.142	T	T	.	0.078	0.093	0.319	2.5	.
P	N	T	N	0.034	T	T	.	0.059	.	.	2.05	.
N	L	.	N	0.143	T	T	T	0.011	0.245	0.048	.	T
A	.	.	.	0.871	.	.	.	.	.	.	.	.
N	.	.	.	0.33	.	.	.	.	.	.	.	.
N	.	.	.	0.182	T	T	T	0.028	.	0.014	.	.

DEOGEN2_	BayesDel_a	BayesDel_r	ClinPred_p	LIST-S2_pre	CADD_raw	CADD_phre	DANN_sco	fathmm-M	fathmm-XF	Eigen-raw_	Eigen-phre	Eigen-PC-ra
T	.	.	.	.	-1.04	0.006	.	.	.	.	.	.
T	.	.	.	.	-0.711	0.041	.	.	.	.	.	.
T	.	.	.	.	-0.711	0.041	.	.	.	.	.	.
.	.	.	.	.	.	.	.	.	.	.	.	.
.	.	.	.	T	-0.317	0.287	.	.	.	.	.	.
T	T	T	T	T	-0.55	0.093	0.187	N	N	-1.963	0.011	-1.906
T	T	T	T	T	-0.06	1.005	0.459	N	N	-2.089	0.006	-2.103
.	.	.	.	.	.	.	.	.	.	.	.	.
.	.	.	.	.	.	.	.	.	.	.	.	.
.	.	.	.	.	.	.	.	.	.	.	.	.
.	.	.	.	.	5.025	33	.	.	.	.	.	.
T	T	T	T	T	1.561	16.12	0.992	D	N	-0.57	1.042	-0.498
T	.	.	.	T	1.053	12.27	0.89	N	.	.	.	.
.	.	.	.	.	4.806	33	.	.	.	.	.	.
T	T	T	T	T	1.975	19.07	0.955	N	N	-0.232	1.79	-0.561
T	.	.	.	T	1.601	16.38	.	.	.	.	.	.
T	.	.	.	T	1.158	13.3	.	.	.	.	.	.
T	.	.	.	T	0.209	3.23	.	.	.	.	.	.
T	T	T	T	T	-0.257	0.384	0.138	N	N	-1.967	0.011	-1.852
.	.	.	.	T	-0.23	0.441	0.366	N	.	.	.	.
.	.	.	.	.	.	.	.	.	.	.	.	.
T	T	T	T	D	1.867	18.24	0.996	N	N	-0.162	1.986	-0.435
T	T	T	T	T	0.705	8.501	0.5	N	N	-1.163	0.254	-1.311
T	T	T	T	T	-0.023	1.2	0.435	N	N	-1.684	0.039	-1.637
T	T	T	T	T	-0.446	0.154	0.639	N	N	-1.534	0.071	-1.673
.	D	D	.	.	7.929	40	0.998	D	D	1.186	22.543	1.045
T	.	.	.	T	0.78	9.195	0.167	N	.	.	.	.
.	T	T	T	T	1.29	14.32	0.986	N	N	-0.943	0.468	-1.063

Eigen-PC-pl	GenoCanyc	integrated_	GM12878_	H1-hESC_fi	HUVEC_fit(	LINSIGHT	GERP++_NI	GERP++_RS	phyloP100\	phyloP30w	phyloP17w	phastCons1
.	.	.	.	.	.	.	.	.	-8.328	-3.489	-1.339	0
.	.	.	.	.	.	.	.	.	-3.619	-1.636	-2.207	0
.	.	.	.	.	.	.	.	.	-3.619	-1.636	-2.207	0
.	.	.	.	.	.	.	.	.	.	.	.	.
.	.	.	.	.	.	.	.	.	-0.631	-0.813	-1.042	0.001
0.021	0	0.638	0.588	0.574	0.668	.	.	.	0.994	-1.32	-1.235	0.054
0.008	0	0.428	0.547	0.547	0.613	.	1.05	-0.525	-0.852	-0.488	-0.947	0
.	.	.	.	.	.	.	.	.	.	.	.	.
.	.	.	.	.	.	.	.	.	.	.	.	.
.	.	.	.	.	.	.	.	.	.	.	.	.
.	.	.	.	.	.	.	.	.	-0.597	0.002	-0.452	0
1.205	0.999	0.722	0.59	0.59	0.735	.	4.35	3.44	1.09	1.176	0.674	0.876
.	1	0.057	0.063	0.074	0.063	0.079	5.09	4.24	0.246	0.187	-0.165	0
.	.	.	.	.	.	.	.	.	-2.106	-1.454	-1.727	0
1.106	0	0.554	0.588	0.574	0.564	.	1.65	0.572	1.233	0.653	0.449	0.011
.	.	.	.	.	.	.	.	.	1.373	1.176	0.676	0.004
.	.	.	.	.	.	.	.	.	0.964	0.128	-0.174	0.244
.	.	.	.	.	.	.	.	.	0.134	-0.138	-0.774	0.063
0.027	0	0.638	0.67	0.618	0.668	.	2.33	2.33	0.391	0.226	-0.593	0
.	0.489	0.078	0.094	0.084	0.063	0.047	0.046	0.046	-1.863	-1.278	-1.682	0
.	.	.	.	.	.	.	.	.	.	.	.	.
1.311	0	0.487	0.574	0.574	0.564	.	0.585	0.585	1.603	-0.869	0.339	0.004
0.202	0.802	0.487	0.574	0.547	0.564	.	0.762	-0.592	0.287	0.33	0.3	0.015
0.065	0.999	0.534	0.611	0.616	0.584	.	0.771	-0.723	0.053	-0.558	-0.641	0.995
0.057	0.952	0.563	0.563	0.616	0.636	.	3.07	-6.13	-1.394	-0.81	-0.135	0
21.934	1	0.442	0.522	0.522	0.562	.	5.52	5.52	7.749	1.023	0.549	1
.	0	0.054	0.061	0.063	0.057	0.045	.	.	0.198	0.268	0.223	0.002
0.415	0	0.487	0.574	0.574	0.564	.	2.01	1.09	0.585	0.037	-0.296	0.003

phastCons3	phastCons1	bStatistic	Interpro_d	GTEx_V8_g	GTEx_V8_t	cosmic92	CLNALLELE	CLNDN	CLNDISDB	CLNREVSTA	CLNSIG	Otherinfo
0	0	.	.	.	.	.	.	.	.	.	.	1
0	0	.	.	.	.	.	.	.	.	.	.	1
0	0	.	.	.	.	.	.	.	.	.	.	1
.	.	.	.	.	.	.	.	.	.	.	.	1
0.003	0.014	889	Neuroblast	.	.	.	.	.	.	.	.	1
0.019	0.011	751	Pleckstrin_	.	.	.	.	.	.	.	.	1
0	0.004	920	Nuclear_Te	.	.	ID=COSV67	.	.	.	.	.	1
.	.	.	.	.	.	ID=COSV64	389841	not_specifi	MedGen:Cl	criteria_pr	Benign	1
.	.	.	.	.	.	.	.	.	.	.	.	1
.	.	.	.	.	.	.	.	.	.	.	.	1
0.534	0.013	751	GPCR,_rho	VWA5A;OR	Testis;Colo	.	.	.	.	.	.	1
0.107	0.033	711	.	.	.	.	.	.	.	.	.	1
0.002	0.002	976	.	ADPRHL1;C	Spleen;Col	ID=COSV50	.	.	.	.	.	1
0	0.014	969	Serpin_dor	SERPINB3;S	Testis;Esop	.	.	.	.	.	.	1
0.001	0.003	964	Methyl-Cp(	.	.	ID=COSV99	.	.	.	.	.	1
0.994	0.911	900	.	ZNF285B;Z	Skin_Not_S	.	.	.	.	.	.	1
0.212	0.241	900	Krueppel-a	ZNF285B;Z	Brain_Fron	.	.	.	.	.	.	1
0.004	0.017	884	.	ZNF285B;Z	Skin_Not_S	.	.	.	.	.	.	1
0.211	0.021	915	.	.	.	ID=COSV56	.	.	.	.	.	1
0	0	641	.	.	.	.	.	.	.	.	.	1
.	.	.	.	.	.	.	.	.	.	.	.	1
0.017	0.305	.	GPCR,_rho	0	Thyroid;Tes	ID=COSV53	.	.	.	.	.	1
0.006	0.004	.	.	0	Whole_Blo	.	.	.	.	.	.	1
0.031	0.025	.	.	0	Whole_Blo	ID=COSV58	.	.	.	.	.	1
0	0.001	934	.	.	.	.	.	.	.	.	.	1
0.999	0.999	721	Calponin_h	.	.	.	.	.	.	.	.	1
0.003	0.003	904	.	.	.	ID=COSV58	.	.	.	.	.	1
0.004	0.014	988	SPATA31/F	.	.	ID=COSV66	.	.	.	.	.	1

1	1	1	1	1	1	1	1	1	1	1	1	
830.06	19	chr1	13223492	.	A	G	830.06	.	AC=2;AF=1	GT:AD:DP:(	1/1:0,19:19:57:844,57,	
830.06	19	chr1	13223511	.	T	C	830.06	.	AC=2;AF=1	GT:AD:DP:(	1/1:0,19:19:57:844,57,	
830.06	19	chr1	13223511	.	T	C	830.06	.	AC=2;AF=1	GT:AD:DP:(	1/1:0,19:19:57:844,57,	
822.06	21	chr1	1.2E+08	.	T	G	822.06	.	AC=2;AF=1	GT:AD:DP:(	1/1:0,21:21:63:836,63,	
78.14	4	chr1	1.49E+08	.	T	C	78.14	.	AC=2;AF=1	GT:AD:DP:(	1/1:0,4:4:12:92,12,0	
158.97	6	chr10	45826906	.	G	C	158.97	.	AC=2;AF=1	GT:AD:DP:(	1/1:0,6:6:18:173,18,0	
280.06	10	chr10	87234695	.	G	A	280.06	.	AC=2;AF=1	GT:AD:DP:(	1/1:0,10:10:30:294,30,	
1290.06	45	chr10	95068566	.	T	C	1290.06	.	AC=2;AF=1	GT:AD:DP:(	1/1:0,45:45:99:1304,1	
737.01	74	chr11	1629969	.	A	AGGCTGTG	737.01	.	AC=2;AF=1	GT:AD:DP:(	1/1:0,74:74:99:2819,2	
3940.03	95	chr11	71527629	.	C	CCTGCTGC(	3940.03	.	AC=2;AF=1	GT:AD:DP:(	1/1:2,93:95:99:3954,1	
3265.06	110	chr11	1.24E+08	.	C	G	3265.06	.	AC=2;AF=1	GT:AD:DP:(	1/1:0,110:110:99:3279	
2063.06	66	chr11	1.25E+08	.	G	A	2063.06	.	AC=2;AF=1	GT:AD:DP:(	1/1:0,66:66:99:2077,1	
112.14	4	chr13	1.13E+08	.	G	A	112.14	.	AC=2;AF=1	GT:AD:DP:(	1/1:0,4:4:12:126,12,0	
4363.06	142	chr18	63712604	.	G	T	4363.06	.	AC=2;AF=1	GT:AD:DP:(	1/1:0,142:142:99:4377	
200.02	7	chr19	7032419	.	G	C	200.02	.	AC=2;AF=1	GT:AD:DP:(	1/1:0,7:7:21:214,21,0	
3377.06	103	chr19	44477666	.	G	C	3377.06	.	AC=2;AF=1	GT:AD:DP:(	1/1:0,103:103:99:3391	
2829.06	92	chr19	44479350	.	G	C	2829.06	.	AC=2;AF=1	GT:AD:DP:(	1/1:0,92:92:99:2843,2	
2425.06	84	chr19	44497294	.	A	G	2425.06	.	AC=2;AF=1	GT:AD:DP:(	1/1:0,84:84:99:2439,2	
216.04	8	chr2	1.12E+08	.	C	A	216.04	.	AC=2;AF=1	GT:AD:DP:(	1/1:0,8:8:24:230,24,0	
37.32	2	chr20	18630471	.	G	T	37.32	.	AC=2;AF=1	GT:AD:DP:(	1/1:0,2:2:6:49,6,0	
98.84	3	chr21	46152330	.	G	A	98.84	.	AC=2;AF=1	GT:AD:DP:(	1/1:0,3:3:9:112,9,0	
4096.06	153	chr22	15528913	.	C	T	4096.06	.	AC=2;AF=1	GT:AD:DP:(	1/1:4,149:153:99:4110	
1320.06	43	chr22	16783675	.	G	T	1320.06	.	AC=2;AF=1	GT:AD:DP:(	1/1:0,43:43:99:1334,1	
1819.06	58	chr22	16784234	.	A	C	1819.06	.	AC=2;AF=1	GT:AD:DP:(	1/1:0,58:58:99:1833,1	
5127.06	169	chr22	25039061	.	G	T	5127.06	.	AC=2;AF=1	GT:AD:DP:(	1/1:0,169:169:99:5141	
19389.06	651	chr3	58008784	.	C	T	19389.06	.	AC=2;AF=1	GT:AD:DP:(	1/1:0,651:651:99:1940	
240.04	8	chr7	76533992	.	T	A	240.04	.	AC=2;AF=1	GT:AD:DP:(	1/1:0,8:8:24:254,24,0	
1644.06	53	chr9	39358957	.	C	T	1644.06	.	AC=2;AF=1	GT:AD:DP:(	1/1:1,52:53:99:1658,1	

,0
,0
,0
,0

,0
35,0
21,0
95,0
,330,0
95,0

',426,0

.,307,0
76,0
52,0

),342,0
29,0
74,0
.,501,0
)3,1949,0

31,0

Appendix B: Supplementary Table 2: Homozygous and compound heterozygous variants in *FLNB* causing SCT

Variant	Variant type	Pathogenecity	Zygosity	Accession	Reference
c.28G>T p.(Glu10Ter)	Stop-gain	Pathogenic	Homozygous	-	Salian et al., 2018
c.220C>T p.(Gln74Ter)	Stop-gain	Pathogenic	Homozygous	-	This study
c.1429delinsCT p.(Val477LeufsX2)	Framshift	Pathogenic	Homozygous	-	Salian et al., 2018
c.1204delG (p.Val402fs)	Deletion	Pathogenic	Homozygous	SCV002053948.1	Submitted by Kasturba Medical College, Manipal, India: https://www.ncbi.nlm.nih.gov/clinvar/variation/1332815/ Salian et al., 2018
c.1243C>T (p.Arg415Ter)	Stop-gain	Pathogenic	Homozygous	SCV002053837.1	Submitted by Kasturba Medical College, Manipal, India: https://www.ncbi.nlm.nih.gov/clinvar/variation/1332749/ Salian (2018) Clin Genet 94, 159; Salian et al., 2018
c.1429delinsCT (p.Val477fs)	Indel/ termination	Pathogenic	Homozygous	SCV002054000.1	Submitted by Kasturba Medical College, Manipal, India: https://www.ncbi.nlm.nih.gov/clinvar/variation/1332844/
c.1493delA (p.Glu498fs)	Deletion/ termination	Pathogenic	Homozygous	SCV002053989.1	Submitted by Kasturba Medical College, Manipal, India: https://www.ncbi.nlm.nih.gov/clinvar/variation/1332839/ Salian et al., 2018
c.1592dup (p.His532fs)	Duplication/ termination	Pathogenic	Homozygous	RCV000782185	Salian et al., 2018
c.1945C>T (p.Arg649Ter)	Stop-gain	Pathogenic	Homozygous	VCV000021280	Krakow et al., 2004
c.1945C>T (p.Arg649Ter)	Stop-gain	Pathogenic	Compound heterozygous*	VCV000021280	Farrington-Rock et al., 2008
c.2452C>T (p.Arg818Ter)	Stop-gain	Pathogenic	Compound heterozygous**	RCV000006768	Submitted by OMIM https://www.ncbi.nlm.nih.gov/clinvar/variation/6396/ Krakow et al., 2004
c.2911dupG (p.Ala971fs)	Duplication/ termination	Pathogenic	Homozygous	VCV002190805	Yasin et al. 2021
c.4671G>A (p.Ser1505ArgfsX33)	Termination	Pathogenic	Compound heterozygous*	-	Farrington-Rock et al., 2008
c.4819C>T (p.Arg1607Ter)	Stop-gain	Likely pathogenic	Compound heterozygous**	RCV000006769	Submitted by Johns Hopkins Genomics, Johns Hopkins Univ. Krakow et al., 2004
c.5548G>T (p.Gly1850Ter)	Stop gain	Pathogenic	Homozygous	RCV000006777	Brunetti-Pierri et al. (2008)
c.5917G>A (p.Glu1973Lys)	single nucleotide variant	Uncertain significance		SCV002786225.1	Submitted by Fulgent Genetics, Fulgent Genetics https://www.ncbi.nlm.nih.gov/clinvar/variation/346353/
c.6010C>T (p.Arg2004Ter)	Stop-gain	Pathogenic	Homozygous	RCV000006776	Submitted by OMIM https://www.ncbi.nlm.nih.gov/clinvar/variation/6407/ Mitter et al., 2008; Farrington-Rock et al., 2008
c.6317delC	Deletion	Pathogenic			Salian et al., 2018
c.6408delC (p.Ser2137fs)	Deletion	Pathogenic	Homozygous	RCV000006767	Submitted by OMIM https://www.ncbi.nlm.nih.gov/clinvar/variation/6395/ Krakow et al., 2004
c.7029 T>G (p.Tyr2343Ter)	Stop-gain	Pathogenic	Homozygous	VCV000021297	Krakow et al., 2004
c.7621dupG (p.Ser2542Leufs*82)	Duplication	Pathogenic	Homozygous	-	Yang et al., 2017

FLNB (NM_001457.4)

*, compound heterozugous detected in patient

**, compound heterozugous detected in patient

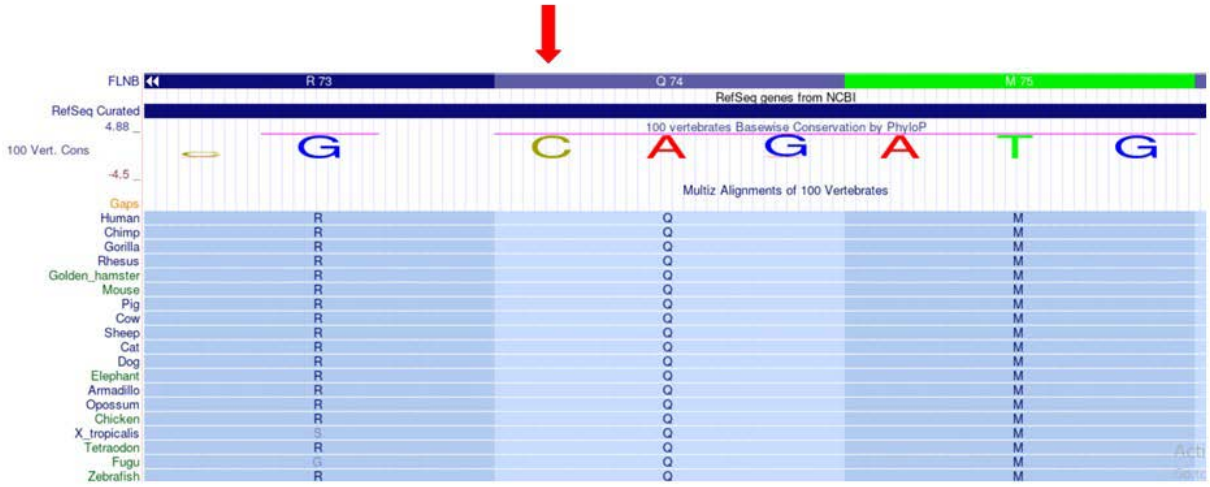

Supplemental Figure 1. The identified variant c.220C>T in FLNB depicted on Vertebrate Multiz Alignment & Conservation Track of UCSC Genome Browser.